

# Charged-Current Reactions and Strangeness: Opportunities at the EIC

Presented at the CFNS Ad Hoc Workshop on  
Opportunities with Heavy Flavor at the EIC

(With thanks and gratitude to the EIC User Community,  
especially the EIC heavy flavor community)

Stephen Sekula<sup>1</sup>

<sup>1</sup>Southern Methodist University, Dallas, TX;

November 4, 2020



**SMU** | DEDMAN COLLEGE  
OF HUMANITIES & SCIENCES

## Outline

### Physics Motivations

Past experiments and current knowledge constraints

### (Some) Experimental Approaches at the EIC

SIDIS or Charm Jets? (why not both!)

Charm Jets and Strangeness: ZEUS/HERA-II

Charm Jets at the EIC: Collider and Detector Perspectives

Charm Jets at the EIC: Modelling CC DIS

Reconstructing and Tagging Charm Jets

Potential impact of Charm Jets on Strangeness

### Conclusions and Outlook

### Appendix

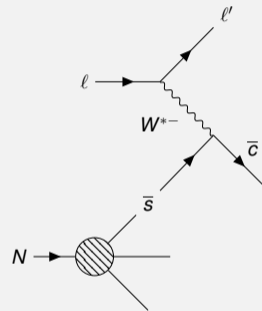
# Physics Motivations

The background features a complex, abstract design. It consists of several overlapping, semi-transparent circles in shades of purple and blue, creating a layered, tunnel-like effect. In the center, there is a bright yellow cone that tapers towards the right. From the base of this cone, numerous thin lines radiate outwards in various colors, including blue, red, and purple, some appearing as solid lines and others as dotted lines. The overall aesthetic is scientific and futuristic.

## Physics Process of Interest - Charged-Current Scattering

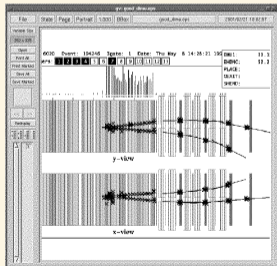
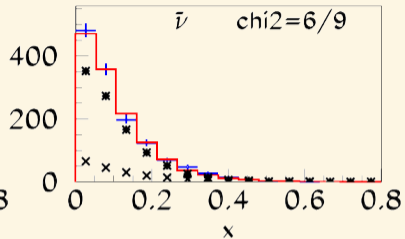
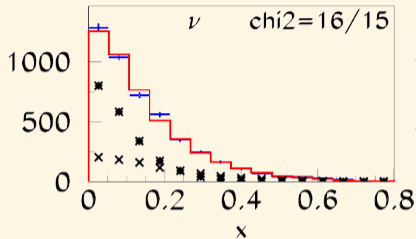
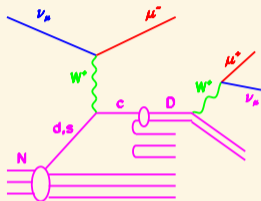


### Feynman Diagram for CC DIS



A greatly improved understanding of the quark sea in nucleons, especially at high  $x$ , is a key science driver for the EIC program. Charged-Current (CC) Deep Inelastic Scattering (DIS) offers one tool for probing the sea. An obvious target here is the strange quark, whose contributions (e.g.  $s(x, Q^2)$  and helicity) are still poorly constrained (especially at high  $x$ ).

## EXAMPLE: Neutrino scattering on a fixed target (NuTeV) [1]



The dimuon signal is very experimentally clean, and thanks to Cabibbo suppression the inference that the preceding charm production is dominated by  $s \rightarrow c$  transitions is safe; the interpretation of the underlying strange sea is challenging due to nuclear corrections and fragmentation/hadronization functions that are convoluted with the underlying PDFs.

Experimental data from this and many other similar experiments have been a key part of PDF fits in recent decades.

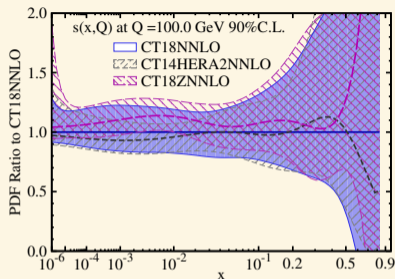
## Constraints on our understanding of $s(x, Q^2)$

### Some Definitions

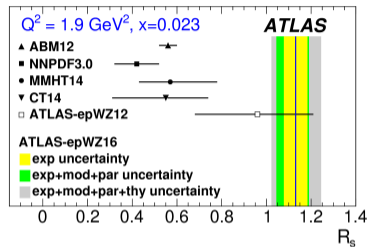
$$r_s = \frac{s + \bar{s}}{2\bar{d}}$$

$$R_s = \frac{s + \bar{s}}{\bar{u} + \bar{d}}$$

The above are functions of  $x$  and  $Q^2$



Example: CT18 PDF uncertainty on  $s(x, Q^2)$  vs.  $x$  [2]

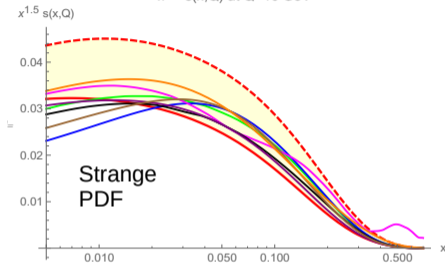


Example: LHC Heavy Ion  $W/Z$  production [3] constraint on  $R_s$

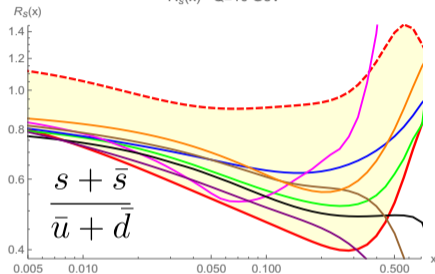
Dimuon measurements in  $\nu$  DIS typically prefer a low value of  $R_s$ ; kaon semi-inclusive DIS typically prefers an even lower value; LHC electroweak boson measurements prefer a value consistent with unity  $\rightarrow$  **while theoretical improvements are definitely being made, we as a community benefit immensely from new data to fuel additional progress.**

# $R_s$ and $s(x, Q^2)$ across several PDF sets

$x^{1.5} s(x, Q)$  at  $Q=10$  GeV



$R_s(x)$   $Q=10$  GeV



- CT18RsLow
- - - CT18RsHigh
- MSTW2008nlo68cl
- nCTEQ15FullNuc\_208\_82
- NNPDF31\_nlo\_as\_0118
- CJ15nlo
- CT18NLO
- EPPS16nlo\_CT14nlo\_Pb208
- HERAPDF20\_NLO\_VAR

$\kappa(Q)$  sorted

| PDF Set                 | $\kappa(Q)=\int R_s(Q)$ |
|-------------------------|-------------------------|
| <b>CT18RsLow</b>        | <b>0.33</b>             |
| CT18NLO                 | 0.38                    |
| CJ15nlo                 | 0.40                    |
| MSTW2008nlo68cl         | 0.43                    |
| EPPS16nlo_CT14nlo_Pb208 | 0.46                    |
| nCTEQ15FullNuc_208_82   | 0.47                    |
| NNPDF31_nlo_as_0118     | 0.54                    |
| HERAPDF20_NLO_VAR       | 0.55                    |
| <b>CT18RsHigh</b>       | <b>0.96</b>             |

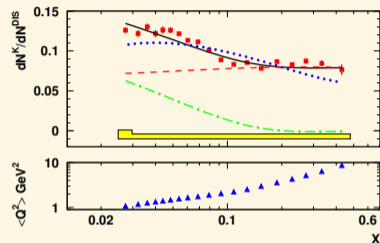
# The Potential of the EIC: Approaches to Strangeness



## Experimental Approaches at the EIC

There are some obvious approaches available to experiments at the EIC for probing the strange quark content and structure of the proton:

- ▶ Semi-Inclusive Deep Inelastic Scattering (SIDIS)
  - ▶ Employ approaches [4] like those at HERMES [5] and COMPASS [6] (for example) to reconstruct single kaons resulting from lepton-nucleon scattering.
  - ▶ Advantages
    - ▶ **Experimental Simplicity:** depending on the detector, you have full reconstruction and/or identification. Also, DIS variables directly accessible to experiment using the scattered beam lepton from neutral current DIS.
    - ▶ **Experimental Cleanliness:** focusing on single well-identified particles can provide a strong advantage in signal-to-noise in the reconstruction.
  - ▶ Drawbacks
    - ▶ **Theoretical Challenge:** the fragmentation function/hadronization model becomes (strongly) entangled in the interpretation of the underlying PDF.

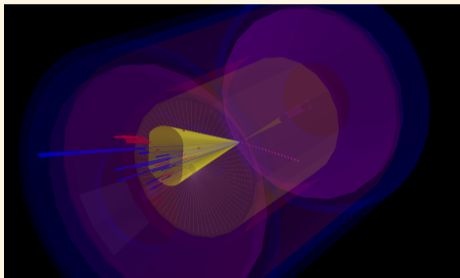


Example: HERMES measurement of kaon multiplicity vs.  $x$  [5] (nuclear-polarized deuteron gas target, positron beam, DIS)

## Experimental Approaches at the EIC

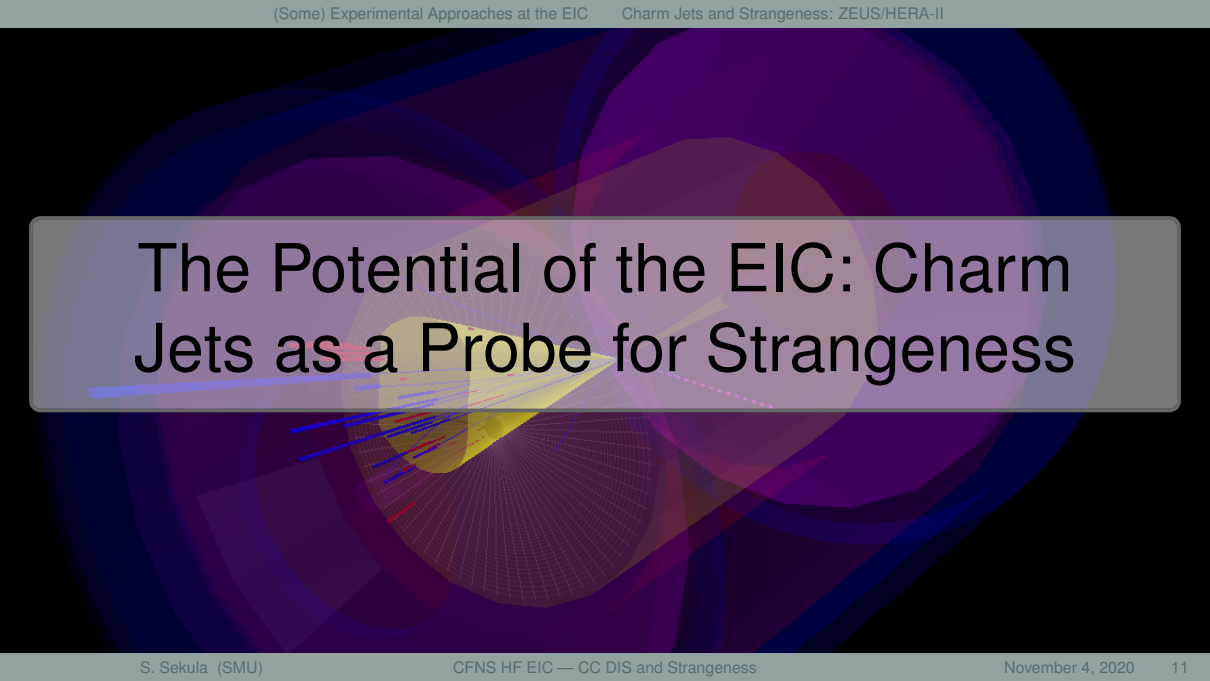
There are some obvious approaches available to experiments at the EIC for probing the strange quark content and structure of the proton:

- ▶ Charm Jet Reconstruction and Tagging
  - ▶ Employ approaches [7] like those at ZEUS (for example) to reconstruct and flavor tag whole jets from  $\bar{s} \rightarrow \bar{c}$  in charged-current (CC) DIS
  - ▶ Advantages
    - ▶ **Theoretically Simpler:** A bit more theoretically straight-forward: no fragmentation function dependence, since the jet is reconstructed.
  - ▶ Drawbacks
    - ▶ **Experimental Complexity:** jet reconstruction and calibration depend on detector design; missing energy reconstruction similarly influenced; flavor tagging depends on good tracking resolution and hermeticity; particle ID depends on dedicated systems and detector design; DIS variables accessible through, for instance, the Jacquet-Blondel approach (degraded resolution).



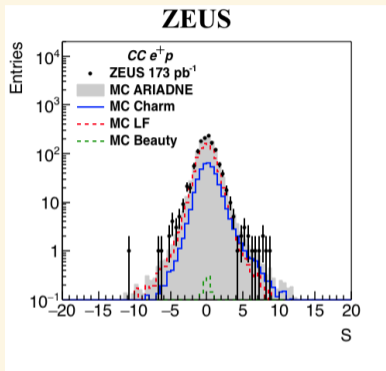
A 3-D visualization of an EIC-like detector, including a CC DIS event with a true charm-initiated and reconstructed jet (yellow cone)

# The Potential of the EIC: Charm Jets as a Probe for Strangeness



## Charm Jets: The ZEUS Experimental Approach [8]

- ▶ HERA-II  $e^\pm p$  collision data,  $\sqrt{s} = 318$  GeV,  $\mathcal{L}_{e^+} = 173\text{pb}^{-1}$ , and  $\mathcal{L}_{e^-} = 185\text{pb}^{-1}$
- ▶ Tracking capabilities included a microvertex detector in addition to the central tracking detector
- ▶ Calorimetry based on a uranium-scintillator design with EM and HAD capabilities



Reconstruct jets ( $k_T$ ,  $R=1$ ) from energy flow objects and identify charm jets using displaced secondary vertex (SVX) counting. Fit to flight information of SVXs.

$$\sigma_{CEW}^+ = 8.5 \pm 5.5(\text{stat.}) \pm {}^{+0.2}_{-1.3}(\text{syst.}) \text{ pb}$$

$$\sigma_{CEW}^- = -5.7 \pm 7.2(\text{stat.}) \pm {}^{+1.0}_{-1.2}(\text{syst.}) \text{ pb}$$

Statistical uncertainties dominate  $\rightarrow$  expect that to be vastly reduced by the high-luminosity program at the EIC.

Dominant systematic uncertainties were from secondary vertex corrections and predictions of the QCD charm contribution; sub-dominant systematics arose from light-flavor background estimation, selection efficiency, and jet energy scale.

## Collider Configuration[12] and Physics Goals (c.f. [7])

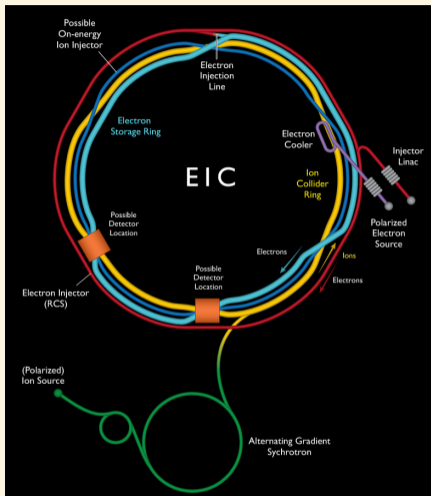
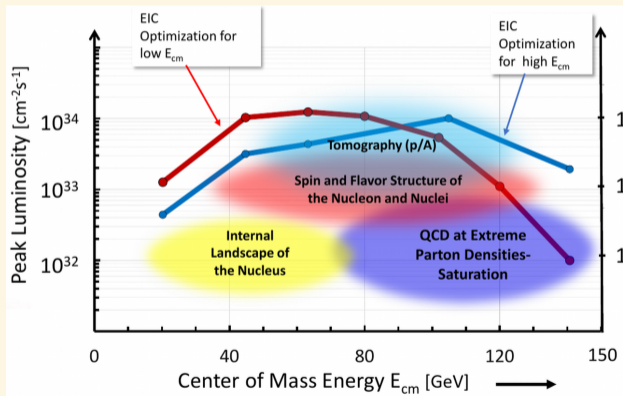
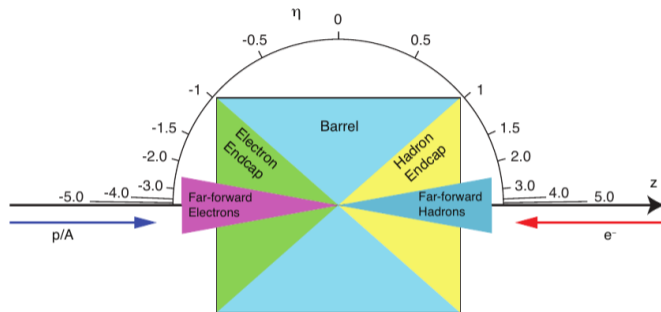


Image from Ref. [9]

The electron-hadron beam model employed for the studies shown here is an  $e^-$  and  $p^+$  collision with  $E_e = 10$  GeV and  $E_p = 275$  GeV. This achieves  $\sqrt{s} = \sqrt{4E_e E_p} \approx 105$  GeV, high instantaneous luminosity, and can yield  $\approx 100 \text{ fb}^{-1}/\text{year}$  [10, 11].



## Delphes and Detector Implementation[12]



Utilizing Delphes detector implementation [13][14] based on EIC Detector Matrix [15]. See Appendix slides 30-31 for detailed breakdown.

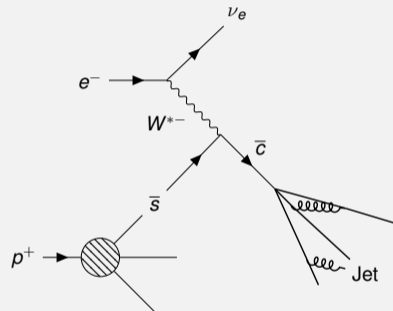
- ▶ Tracking: covers  $|\eta| < 3.5$  with 85%-98% efficiency depending on  $p_T$  and  $\eta$ ; track impact parameter resolution is  $20\mu\text{m}$  in  $d_0$  and  $z_0$ . Tracking system immersed in 1.5T magnetic field.
- ▶ ECal covers  $|\eta| < 4$  with resolution of  $\sigma = E \times (1.0\%) \oplus \sqrt{E} \times (2.0\%)$  in the backward direction worsening to  $E \times (2.0\%) \oplus \sqrt{E} \times (12.0\%)$  in the forward direction. Granularity is  $(\Delta\eta, \Delta\phi) = (0.020, 0.020)$ .
- ▶ HCal covers  $|\eta| < 4$  with resolution of  $\sigma = E \times (10\%) \oplus \sqrt{E} \times (50\%)$  in the backward and forward direction, worsening to  $E \times (10.0\%) \oplus \sqrt{E} \times (100\%)$  in the barrel. Granularity is best in forward/backward region,  $(\Delta\eta, \Delta\phi) = (0.025, 0.025)$ , and more coarse in the barrel,  $(\Delta\eta, \Delta\phi) = (0.1, 0.1)$

## Modeling CC DIS



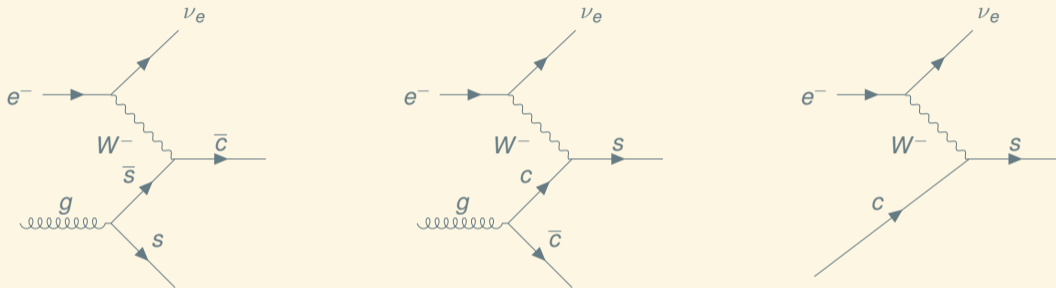
- ▶ Charged-Current (CC) DIS is simulated using PYTHIA8 [16, 17]
  - ▶ Process: `WeakBosonExchange:ff2ff(t:W)`
  - ▶  $Q^2 > 100 \text{ GeV}^2$
  - ▶  $\sigma_{Q^2 > 100 \text{ GeV}^2}^{\text{PYTHIA8}} = 14.76 \text{ pb}$
- ▶ PDF set: CT18 from LHAPDF; baseline is CT18NNLO
- ▶ Generated 20M events for study (using varying amounts of this for the parts of this talk)

### Feynman Diagram for CC DIS



## Broader View of Charm Jet Production at the EIC

The CC DIS process  $W^- \bar{s} \rightarrow \bar{c}$  is, of course, not the only contributor to charm jet production at an electron-hadron machine [8].

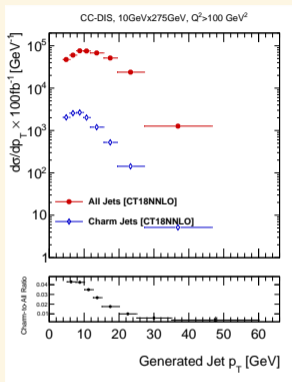


**LEFT DIAGRAM:** modelled in PYTHIA8 for this study. Reported cross-section is  $\sigma_{Q^2 > 100 \text{ GeV}^2}^{\text{PYTHIA8}} = 14.76 \text{ pb}$ .

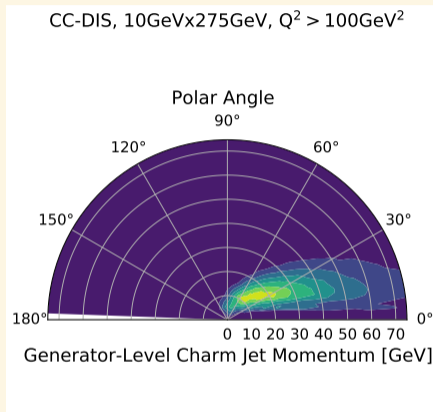
**MIDDLE AND RIGHT DIAGRAMS:** Gluon splitting and charm-initiated graphs are also important contributors, being sensitive to  $g(x, Q^2)$  and  $F_2^{c\bar{c}}$  (including a possible nonperturbative charm component); these were not modeled in this study. Also (not shown) need to consider final-state gluon radiation,  $g \rightarrow c\bar{c}$ . These components need to be disentangled in a full-scale data analysis. They are ignored here and will be considered in future work (this leads to a conservative underestimate of the charm jet yield for this study).



## Differential Cross Sections and Yields for $100\text{fb}^{-1}$



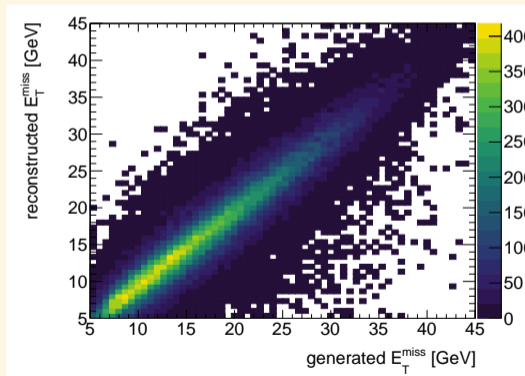
Theoretical expectation is for thousands of charm jets produced in  $100\text{fb}^{-1}$  from CC DIS (a few percent of the total CC DIS jet yield).



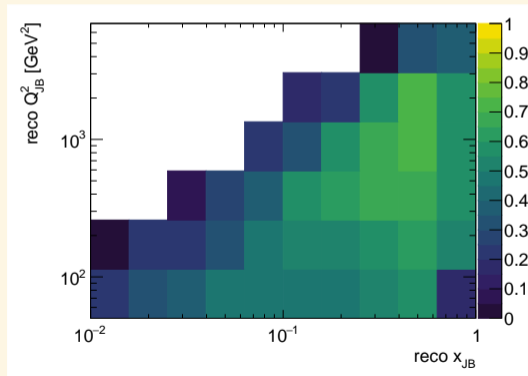
Charm jets (anti- $k_T$ ,  $R=1$ ) preferentially produced at low-angle ( $\theta \approx 35^\circ$  or  $\eta \approx 1.2$ , approximately the transition region between barrel and hadronic endcap) but span out to  $\eta \approx 3.5 - 4.0$ . Need good tracking and calorimetry coverage (and hermeticity!) down to low forward angles to insure reliable reconstruction of these jets.

## Jets and Missing Transverse Energy

Jets are reconstructed using a particle flow algorithm, taking advantage of the tracking information to improve our knowledge of the final reconstructed jet. No effort at calibration or jet energy scale estimation is made here, but we would assume a final 10% (or so) systematic error assuming a typical modern detector technology and geometry configuration. Good jet calibration is essential to MET reconstruction (left) and the purity of the Jacquet-Blondel computation of  $Q^2$  and  $x$  (right).

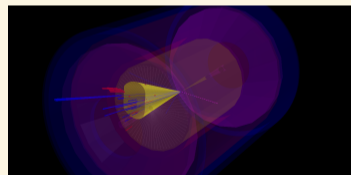
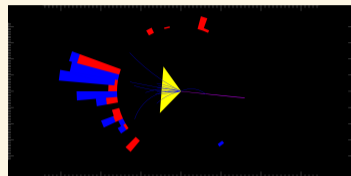
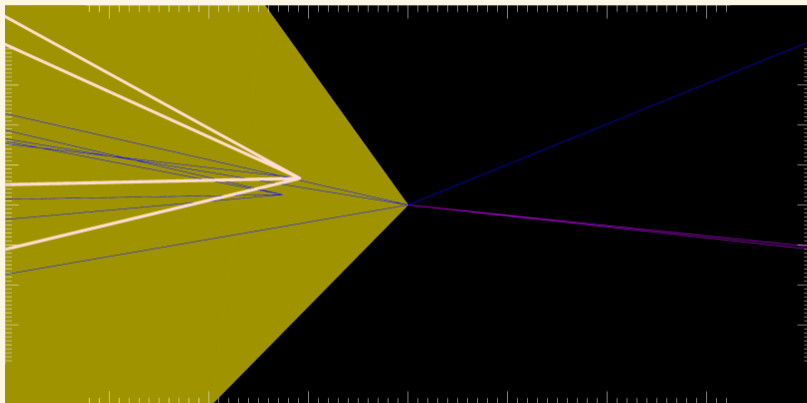


Jet energy resolution



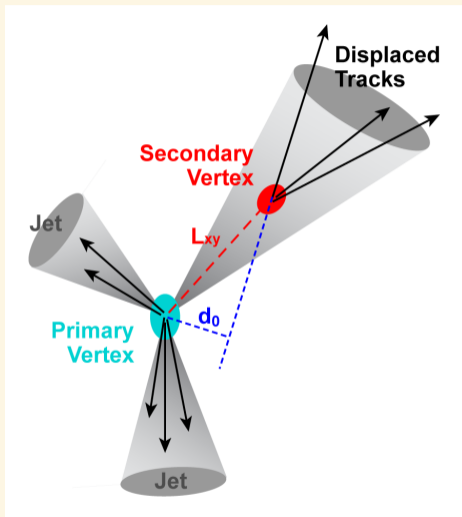
JB  $x$  and  $Q^2$  purity

**Example: Event Display of Charm Jet, 8 high-IP tracks,  $E_T^{miss} = 24.7$  GeV,**  
 $p_T = 24.5$  GeV,  $\eta = 1.6$



The displaced vertices in this jet (there are 2; 1 is highlighted) are about 0.5mm from the IP in  $x - y$  plane. The jet was truth-matched to a charm jet and charm-tagged. Two true kaons are present, one emerging from each displaced vertex. Good case for jet-level tagging but also inclusion of track-level particle identification (PID) in an inclusive tagging algorithm.

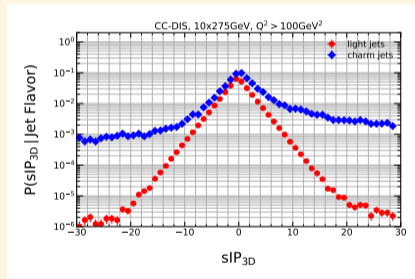
## Flavor-Tagging Jets: An Example Using High-Impact Parameter Track Counting



Graphic from ATLAS b-jet Trigger Signature Group

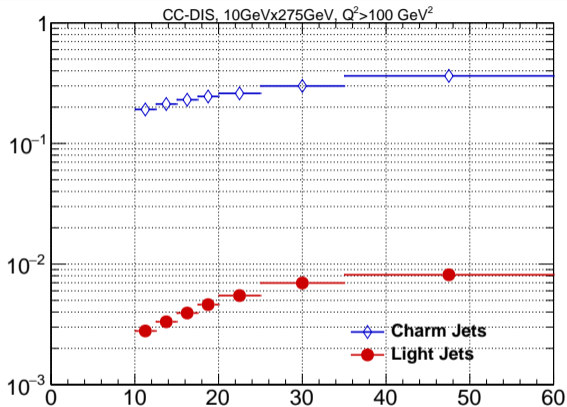
Delphes provides a nice, basic flavor tagging algorithm: high-impact-parameter track counting inside a jet object. The *signed 3-D impact-parameter* is defined as:

$$sIP_{3D} = \text{sgn}(\vec{p}_j \cdot \vec{L}) \times \sqrt{(d_0/\sigma_{d_0})^2 + (z_0/\sigma_{z_0})^2} \quad (1)$$



We optimize hyper-parameters by minimizing the uncertainty on the final light-jet-subtracted charm jet yield: track  $p_T^{min} = 0.5 \text{ GeV}$ ;  $sIP_{3D} > 3$  per track;  $\geq 2$  such tracks.

## Flavor Tagging Efficiency



Track counting efficiency on charm (light) jets ranges averages to 20% (0.4%).

At this level of efficiency, and given the CC DIS production cross-section and the high efficiency of selecting events with a jet (95%) and with  $E_T^{miss} > 10\text{ GeV}$  (75%), we expect  $\sim 6000$  events in  $100\text{ fb}^{-1}$  at the EIC (1 year of data-taking).

Modern state-of-the-art charm jet tagging approaches (multivariate in nature, employing track, vertex, and particle ID information) achieve charm (light) efficiencies of  $\approx 40\%$  (0.5%). We can expect this to be better with more exploratory effort, so this is conservative for now.

**SIDE NOTE:** Adding kaon, electron, and muon PID to the tagging approach was studied  $\rightarrow$  anticipate 50% gains in charm jet efficiency with negligible impact on background rate. This approach is not used for the results on the next slides.

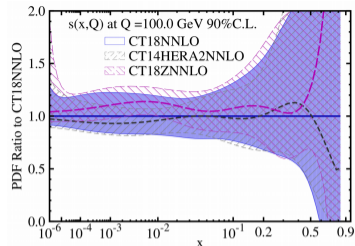
## nucleon strangeness remains comparatively less constrained

- in CT, main inputs are from  $\nu$ DIS on heavy nuclei (nuclear corr. relevant)
- of interest: the strange suppression ratio,  $R_s = \frac{s + \bar{s}}{\bar{u} + \bar{d}}$
- typical QCD fits find  $R_s \sim 0.5$ ; ATLAS W/Z production favors  $R_s \sim 1$

→ **question: can CC charm jet production off proton distinguish small from large  $R_s$ ?**

- Lagrange multiplier scans of  $R_s$  in CT18 analysis:

arXiv: 1912.10053 [hep-ph]

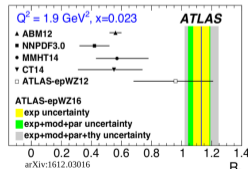
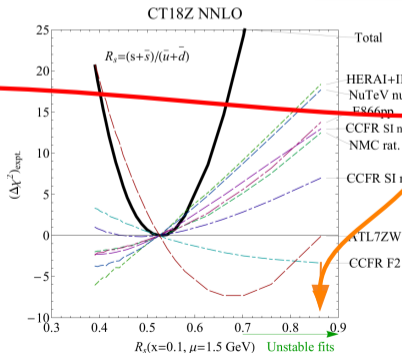
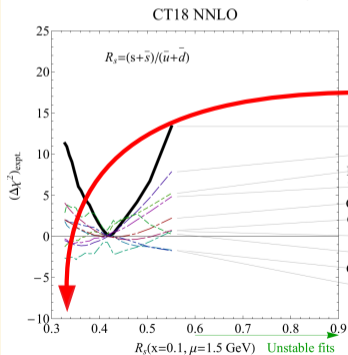


### theory inputs: for

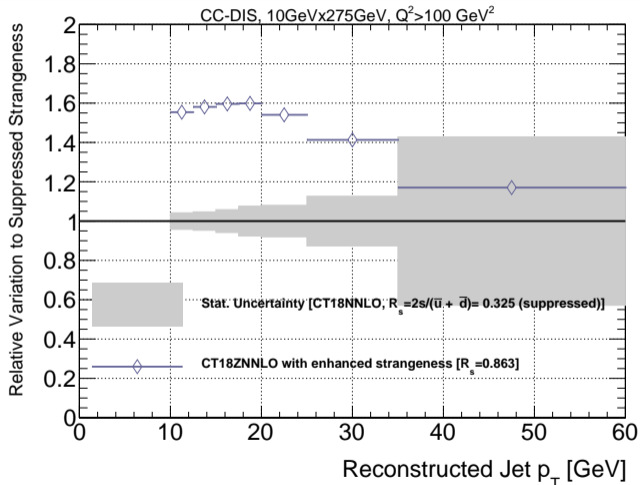
$x = 0.1, \mu = 1.5$  GeV

\*  $R_s = 0.325$  (CT18)

\*  $R_s = 0.863$  (CT18Z)



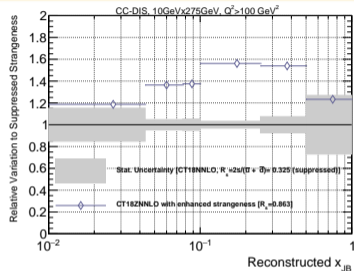
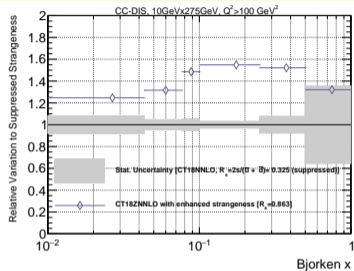
## Statistical Uncertainty ( $100 \text{ fb}^{-1}$ ) vs. current theory uncertainty on Strangeness in the Proton



Compare two variations of the CT18 PDFs: CT18NNLO with suppressed strangeness ( $R_s = \frac{2s}{\bar{u} + \bar{d}} = 0.325$ ) and CT18ZNNLO with enhanced strangeness ( $R_s = 0.863$ ). The variation in charm jet yields from these two cases vastly exceed statistical uncertainty on the worst-case (suppressed) scenario!

Even considering obvious missing uncertainties like jet energy scale ( $\sim 10\%$ ), selection and other detector systematics, and the fact that we think this charm tagging efficiency is conservatively underestimated (we've only employed a single method - mature taggers use a multivariate combination of multiple approaches, including the one used here), this has the promise of greatly improving our knowledge of the strange PDF.

# Statistical Uncertainty ( $100 \text{ fb}^{-1}$ ) vs. current theory uncertainty on Strangeness in the Proton



We show here the same comparison of yield uncertainty (grey, suppressed strangeness) to the variation between enhanced and suppressed strangeness in the proton (blue markers), but for true Bjorken  $x$  and for the experimentally inferred "Jacquet-Blondel"  $x$  [19].

Our best experimental sensitivity to the differences between these extrema is anticipated in the region of  $x_{JB} \approx x = [0.05, 0.5]$ .



# Conclusions and Outlook



## Conclusions and Outlook

- ▶ CC DIS has been for a long time a vital tool in probing intrinsic strangeness in the proton.
- ▶ The neutrino beam experiments, kaon semi-inclusive DIS, and LHC data (for example) have improved our knowledge of  $s(x, Q^2)$  but there is so much more to be learned, especially at high- $x$
- ▶ SIDIS and CC DIS will be important tools for the EIC (I've only really talked about CC DIS in this talk)
- ▶ Ultimately, a **global analysis that combines approaches** will be the best way forward for  $s(x, Q^2)$  and our community as a whole → take advantage of the strengths and weaknesses of each approach while gaining from the statistically independent methodologies!
- ▶ Close coordination between experimental and theoretical segments of the community is vital, especially to inform on (a) modeling the EIC collision environment, including EW and QCD backgrounds; (b) disentangling theory contributions to the final state that must be handled to interpret the experimental results.
- ▶ *NOT COVERED IN THIS TALK*: EIC beam polarization provides a vital opportunity to use SIDIS, CC DIS, etc. to probe strangeness helicity and contribution to the nucleon spin.

### Future Directions for CC DIS Work

- ▶ Full secondary vertex reconstruction (ala ZEUS!)
- ▶ Jet substructure for flavor tagging
- ▶ More realistic PID implementation (e.g. specific detector ideas)
- ▶ Improved primary interaction modeling (polarization, backgrounds, etc.)
- ▶ Pseudodata input to PDF fits to test impact of EIC on  $s(x, Q^2)$

An aerial photograph of a university campus. In the background, a large, classical-style building with a prominent green dome and a portico with columns. To the right, another large brick building is visible. In the foreground, a wide, green lawn is crisscrossed by paved walkways. A circular fountain with a central water jet is located in the lower right. Numerous people are seen walking on the paths and sitting on benches. The sky is blue with light clouds.

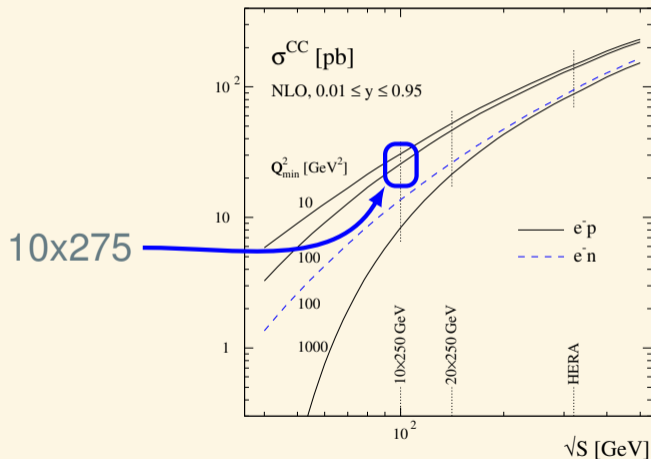
# Appendix

## Approaches and Challenges

Channels listed are increasingly demanding. For every row consider all requirements above as well. The  $(x, Q^2)$  dependence of the observables is omitted for brevity. Table from Miguel Arratia.

| Channel                                   | Observable                    | Goal                              | Physics-driven requirement   | Category  | numbers  |
|---|-------------------------------|-----------------------------------|--|---|--|
| e-jet (NC)<br>100 fb <sup>-1</sup>        | $d\sigma, A_{UT}(\Delta\phi)$ | $k_T$ -dependence of quark Sivers | $\Delta\phi$ res. $\ll$ intrinsic width<br>$R = 1.0 \rightarrow$ had. corr. $O(1)\%$<br>particle-flow reco           | Jet res.<br>Acceptance<br>Granularity                         | jet $dE/E < 15\%$<br>$2\pi,  \eta  < 3.5$ HCAL and ECAL<br>endcap $\Delta\phi \times \Delta\eta \leq 0.025 \times 0.025$   |
| h-in-jet (NC)<br>100 fb <sup>-1</sup>     | $d\sigma, A_{UT}(z_h, j_T)$   | $q$ -transversity                 | + $dp/p$ at high $z <$ jet $dE/E$  | Tracker<br>PID  | $dp/p < 5\%$ at 50 GeV<br>$\eta < 3.5$ and 40 GeV  |
| $\nu$ -jet (CC)<br>100 fb <sup>-1</sup>   | $d\sigma, A_{UT}$             | $u$ Sivers                        | $\Delta\phi \ll 0.3$ rad<br>Bkg. rej. to phot and NC<br><br>>70% survival prob.<br>for 5 bins per-decade in $x, Q^2$ | $E_T^{miss}$ res.<br>Acceptance<br><br>Jet/ $E_T^{miss}$ res. | $dE_T^{miss}/E_T^{miss} < 15\%$<br>$2\pi,  \eta  < 3.5$ HCAL and ECAL<br>$E > 100$ MeV thres. ECAL<br>$E > 400$ MeV thres. HCAL<br>$p_T > 100$ MeV tracker<br>$dx/x < 20\%$ ,<br>$dE_T^{miss}/E_T^{miss} < 15\%$ |
| h-in-jet (CC)<br>100 fb <sup>-1</sup>     | $d\sigma, A_{UT}(z_h, j_T)$   | $u$ -transversity                 | —  | —   | —  |
| c-jet (CC)<br>100 fb <sup>-1</sup>        | $d\sigma, A_{LL}$             | $s$ PDF& helicity                 | charm-tagging  | Tracker<br><br>PID  | c-jet tag at $> 10\%$ ( $< 0.05\%$ )<br>DCA = 20 $\mu\text{m}$ , $\approx 100\%$ eff.<br>TBD   |
| h-in-c-jet (CC)<br>100 fb <sup>-1</sup>   | $d\sigma, A_{UT}(z_h, j_T)$   | $s$ -transversity                 | —  | —   | —  |
| c-jet ( $e^+$ CC)<br>100 fb <sup>-1</sup> | $d\sigma, A_{LL}$             | $s/\bar{s}$ asymmetry             | positrons  | —   | —  |

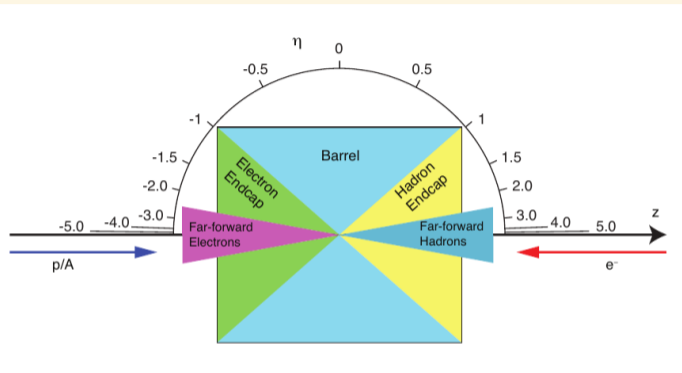
## CC DIS NLO Cross-Section Prediction



Total CC DIS rate at EIC with 10x275 configuration ( $\sqrt{s} = 105$  GeV) is about 20pb.

Figure is from Ref. [20].

## Delphes and Detector Implementation[12]



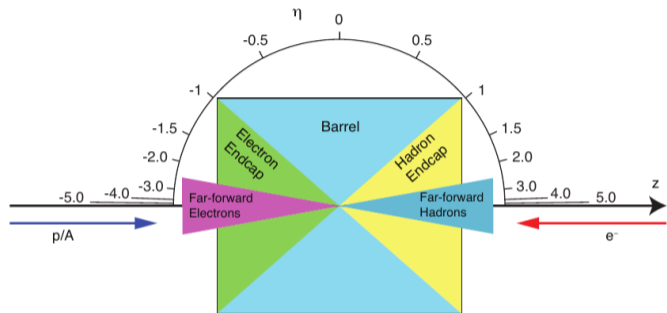
Charged particle tracking covers  $|\eta| < 3.5$  and is efficient for tracks with  $p_T > 0.1 \text{ GeV}$ . **For this study, the track  $d_0$  and  $z_0$  resolution formulas are each set to  $20 \mu\text{m}$  for all  $(p_T, \eta)$  where this tracker model has acceptance.**

- ▶ Implementation in Delphes by Miguel[13] based on EIC Detector Matrix [15]; a fork is used for studies in this talk [14]
- ▶ Consists of a tracking system, ECal, and HCal. Tracker is immersed in 1.5T solenoidal magnetic field.

### Tracker Information

- ▶ For particles below 0.1 GeV in  $p_T$ , or with  $|\eta| > 3.5$ , efficiency is 0.
- ▶ For particles with  $p_T = (0.1, 1.0]$ , efficiency varies from 95% for  $|\eta| \leq 1.5$ , to 92% for  $|\eta| = (1.5, 2.5]$ , to 85% for  $|\eta| = (2.5, 3.5]$ .
- ▶ For particles with  $p_T > 1.0$ , efficiency varies from 98% for  $|\eta| \leq 1.5$ , to 95% for  $|\eta| = (1.5, 2.5]$ , to 90% for  $|\eta| = (2.5, 3.5]$ .

## Delphes and Detector Implementation[12]



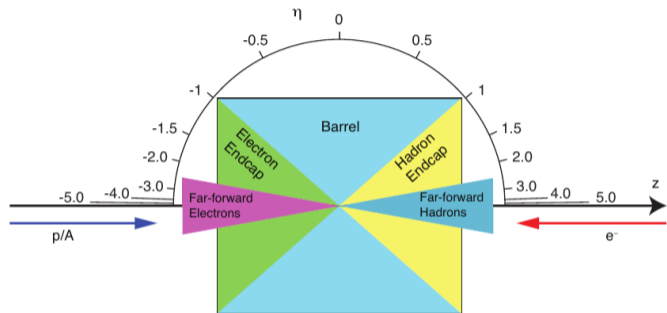
The barrel and endcap electromagnetic calorimeters ( $|\eta| < 1.0$  and  $|\eta| = [1.0, 4.0]$ , respectively) are assumed to have a granularity of  $(\Delta\eta, \Delta\phi) = (0.020, 0.020)$ . The minimum cell energy threshold is set to 0.2 GeV.

- ▶ Implementation in Delphes by Miguel[13] based on EIC Detector Matrix [15]; a fork is used for studies in this talk [14]
- ▶ Consists of a tracking system, ECal, and HCal. Tracker is immersed in 1.5T solenoidal magnetic field.

### ECal Information

- ▶ For  $|\eta| = (-4.0, -2.0]$ ,  
 $\sigma^2 = E^2 \times (1.0\%)^2 + E \times (2.0\%)^2$
- ▶ For  $|\eta| = (-2.0, -1.0]$ ,  
 $\sigma^2 = E^2 \times (1.0\%)^2 + E \times (7.0\%)^2$
- ▶ For  $|\eta| = (-1.0, 1.0]$ ,  
 $\sigma^2 = E^2 \times (1.0\%)^2 + E \times (10.0\%)^2$
- ▶ For  $|\eta| = (1.0, 4.0]$ ,  
 $\sigma^2 = E^2 \times (2.0\%)^2 + E \times (12.0\%)^2$

## Delphes and Detector Implementation[12]



The EIC baseline detector does not describe the granularity of an HCal. (an  $\approx$  sPHENIX HCal is assumed). The barrel hadronic calorimeter ( $|\eta| < 1.0$ ) has  $(\Delta\eta, \Delta\phi) = (0.1, 0.1)$ ; the endcap ( $|\eta| = [1.0, 4.0]$ ) has  $(\Delta\eta, \Delta\phi) = (0.025, 0.025)$ , improved over barrel. Resolution also improves in the endcap. The minimum cell object threshold is set to 0.4 GeV.

- Implementation in Delphes by Miguel[13] based on EIC Detector Matrix [15]; a fork is used for studies in this talk [14]
- Consists of a tracking system, ECal, and HCal. Tracker is immersed in 1.5T solenoidal magnetic field.

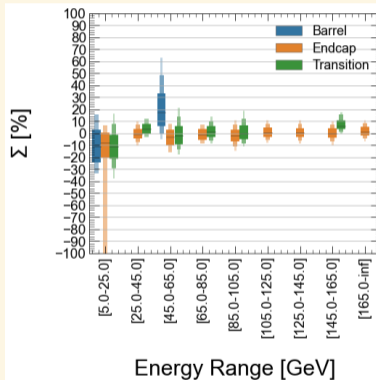
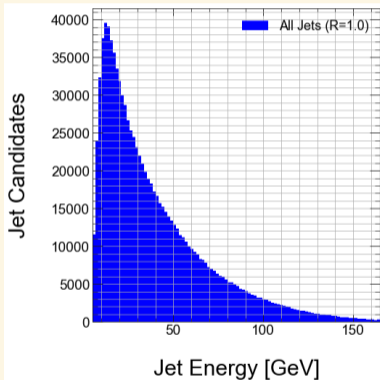
### HCal Information

- For  $|\eta| = (-4.0, -1.0]$ ,  
 $\sigma^2 = E^2 \times (10.0\%)^2 + E \times (50.0\%)^2$
- For  $|\eta| = (-1.0, 1.0]$ ,  
 $\sigma^2 = E^2 \times (10.0\%)^2 + E \times (100.0\%)^2$
- For  $|\eta| = (1.0, 4.0]$ ,  
 $\sigma^2 = E^2 \times (10.0\%)^2 + E \times (50.0\%)^2$



## Validation Plots for Reconstructed Jets (R=1.0)

Jets are reconstructed using tracks and calorimeter clusters in an EnergyFlow approach. The Anti- $k_T$  algorithm builds the jet (R=1.0) and energy flow is used to determine the jet four-vector. The reconstruction implementation comes from FastJet [21, 22].



Jet energy resolution ( $\Sigma \equiv (E_J - E_J^{true})/E_J^{true}$ ) in this detector model varies with jet energy, of course, but generally has an RMS that varies between 15-20% at low  $E_J$  to 5-10% at higher  $E_J$ .

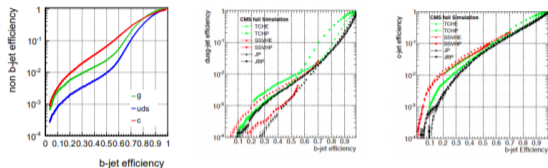
Barrel jet resolution is worse than endcap resolution ( $\sim 20\%$  vs. 7.5 – 15%).

The “Transition” region is the one between the barrel and endcap(s). I set that to be between  $|\eta| = [0.5, 1.5]$  given the size of the jets.

True jets are matched to reconstructed jets if they fall within half the radius parameter of the reconstructed jet axis. Closest in  $\Delta R = \sqrt{(\Delta\phi)^2 + (\Delta\eta)^2}$  is retained.

## Example: Delphes vs. CMS

### Performance : High Purity



- ▶ c mistag rate agrees ok
- ▶ too pessimistic light rejection for low btagging efficiency

At 55% b-tagging efficiency (Medium working point) :

DELPHES : l-mis = 1.5%, c-mis = 10%

CMS : l-mis = 1.0%, c-mis = 10%

$$\text{sig}(IP)_{\min} = 6.5$$

Dedicated charm-jet taggers developed for LHC experiments (e.g. ATLAS) use multivariate discriminants that combine 2-D and 3-D track impact parameter information with secondary vertex and jet evolution information. In their loose (tight) configurations they can select 40% (20%) of charm jets while keeping only 25% (5%) of b-jets and 5% (0.5%) of light jets. That's “state-of-the-art” for now.

Slide from Ref. [23]

## References I

- [1] **NuTeV** Collaboration, M. Goncharov *et al.*, “Precise Measurement of Dimuon Production Cross-Sections in  $\nu_\mu$  Fe and  $\bar{\nu}_\mu$  Fe Deep Inelastic Scattering at the Tevatron.,” *Phys. Rev. D* **64** (2001) 112006, arXiv:hep-ex/0102049.
- [2] T.-J. Hou *et al.*, “New CTEQ global analysis of quantum chromodynamics with high-precision data from the LHC,” arXiv:1912.10053 [hep-ph].
- [3] **ATLAS** Collaboration, M. Aaboud *et al.*, “Precision measurement and interpretation of inclusive  $W^+$ ,  $W^-$  and  $Z/\gamma^*$  production cross sections with the ATLAS detector,” *Eur. Phys. J. C* **77** (2017) no. 6, 367, arXiv:1612.03016 [hep-ex].
- [4] E. C. Aschenauer, I. Borsa, R. Sassot, and C. Van Hulse, “Semi-inclusive Deep-Inelastic Scattering, Parton Distributions and Fragmentation Functions at a Future Electron-Ion Collider,” *Phys. Rev.* **D99** (2019) no. 9, 094004, arXiv:1902.10663 [hep-ph].
- [5] **HERMES** Collaboration, A. Airapetian *et al.*, “Measurement of Parton Distributions of Strange Quarks in the Nucleon from Charged-Kaon Production in Deep-Inelastic Scattering on the Deuteron,” *Phys. Lett. B* **666** (2008) 446–450, arXiv:0803.2993 [hep-ex].

## References II

- [6] **COMPASS** Collaboration, M. Alekseev *et al.*, “Flavour Separation of Helicity Distributions from Deep Inelastic Muon-Deuteron Scattering,” *Phys. Lett. B* **680** (2009) 217–224, [arXiv:0905.2828](https://arxiv.org/abs/0905.2828) [hep-ex].
- [7] M. Arratia, Y. Furlotova, T. Hobbs, F. Olness, and S. J. Sekula, “Charm jets as a probe for strangeness at the future Electron-Ion Collider,” [arXiv:2006.12520](https://arxiv.org/abs/2006.12520) [hep-ph].
- [8] **ZEUS** Collaboration, I. Abt *et al.*, “Charm production in charged current deep inelastic scattering at HERA,” *JHEP* **05** (2019) 201, [arXiv:1904.03261](https://arxiv.org/abs/1904.03261) [hep-ex].
- [9] “The EIC Machine.” <https://www.bnl.gov/eic/machine.php>.
- [10] E. C. Aschenauer, M. D. Baker, A. Bazilevsky, K. Boyle, S. Belomestnykh, I. Ben-Zvi, S. Brooks, C. Brutus, T. Burton, S. Fazio, A. Fedotov, D. Gassner, Y. Hao, Y. Jing, D. Kayran, A. Kiselev, M. A. C. Lamont, J. H. Lee, V. N. Litvinenko, C. Liu, T. Ludlam, G. Mahler, G. McIntyre, W. Meng, F. Meot, T. Miller, M. Minty, B. Parker, R. Petti, I. Pinayev, V. Ptitsyn, T. Roser, M. Stratmann, E. Sichtermann, J. Skaritka, O. Tchoubar, P. Thieberger, T. Toll, D. Trbojevic, N. Tsoupas, J. Tuozzolo, T. Ullrich, E. Wang, G. Wang, Q. Wu, W. Xu, and L. Zheng, “eRHIC Design Study: An Electron-Ion Collider at BNL,” 2014.

## References III

- [11] Ferdinand Willeke, “EIC accelerator and IR design status,” in *2nd EIC Yellow Report Workshop at Pavia University*. 2020. <https://indico.bnl.gov/event/8231/contributions/37060/>.
- [12] E. Aschenauer, A. Kiselev, R. Petti, T. Ullrich, C. Woody, P. Nadel-Turonski, L. Gonella, and P. Jones, “Electron-Ion Collider Detector Requirements and R&D Handbook,” tech. rep., 2019.
- [13] [https://github.com/miguelignacio/delphes\\_EIC](https://github.com/miguelignacio/delphes_EIC).
- [14] [https://github.com/stephensekula/delphes\\_EIC](https://github.com/stephensekula/delphes_EIC).
- [15] “EIC Detector Matrix,” 2020. <https://physdiv.jlab.org/DetectorMatrix/>.
- [16] T. Sjöstrand, S. Mrenna, and P. Skands, “A brief introduction to pythia 8.1,” *Computer Physics Communications* **178** (Jun, 2008) 852867. <http://dx.doi.org/10.1016/j.cpc.2008.01.036>.
- [17] T. Sjöstrand, S. Mrenna, and P. Skands, “Pythia 6.4 physics and manual,” *Journal of High Energy Physics* **2006** (May, 2006) 026026. <http://dx.doi.org/10.1088/1126-6708/2006/05/026>.
- [18] Tim Hobbs, “Update ongoing PDF studies for EIC IRG,” in *2nd EIC Yellow Report Workshop at Pavia University*. 2020. <https://indico.bnl.gov/event/8231/contributions/37765/>.

## References IV

- [19] U. Amaldi *et al.*, “REPORT FROM THE STUDY GROUP ON DETECTORS FOR CHARGED CURRENT EVENTS,” in *ECFA Study of an ep Facility for Europe*, pp. 377–414. 1, 1979.
- [20] E. C. Aschenauer, T. Burton, M. Stratmann, T. Martini, and H. Spiesberger, “Prospects for charged current deep-inelastic scattering off polarized nucleons at a future electron-ion collider,” *Physical Review D* **88** (Dec, 2013) . <http://dx.doi.org/10.1103/PhysRevD.88.114025>.
- [21] M. Cacciari, G. P. Salam, and G. Soyez, “Fastjet user manual,” *The European Physical Journal C* **72** (Mar, 2012) . <http://dx.doi.org/10.1140/epjc/s10052-012-1896-2>.
- [22] M. Cacciari and G. P. Salam, “Dispelling the  $n^3$  myth for the  $k_t$  jet-finder,” *Physics Letters B* **641** (Sep, 2006) 5761. <http://dx.doi.org/10.1016/j.physletb.2006.08.037>.
- [23] CP3 UCL, “Impact parameter b-tagging in DELPHES,” 2104. [https://cp3.irmp.ucl.ac.be/projects/delphes/raw-attachment/wiki/WorkBook/Modules/btagging\\_v2.pdf](https://cp3.irmp.ucl.ac.be/projects/delphes/raw-attachment/wiki/WorkBook/Modules/btagging_v2.pdf).